Vol. 78 No. 3 ACTA GEOLOGICA SINICA June 2004 843-847
http://www.geojournals.cn/dzxbcn/ch/index.aspx

Model of Reflection Spectra of Rock Surface in 2π Space

ZHAO Hongying[1] ZHAO Hu[1], YAN Lei[2] and ZHAO Yunsheng[3]
1 *Institute of Remote Sensing and GIS, Peking University, Beijing 100871;*
E-mail: zhying001@sina.com
2 *Beijing Key Lab of Spatial Information Integration and Its Applications,*
Institute of RS and GIS, Peking University, Beijing 100871
3 *Department of Geography, Northeast Normal University, Changchun, Jilin 130024*

Abstract This paper deals with reflection spectra and polarized reflection spectra of 20 sorts of rock in 2π space, and then creates a model of reflection spectra of rock surface in 2π space. We measured the change of reflection and polarized reflection spectra as altering the incidence angle, vertex angle, azimuth angle, band and polarization. The results show that influence of the incidence angle on spectral curves is very strong. And when the vertex angle is constant, the horizontal azimuth polarizes rock spectra, and distorts the circular spectrum to become elliptic. The polarization influences the reflection intensity of rock spectra, but has no evident influence on the characteristics of wave forms of rock in 2π space. Therefore, we can describe the whole reflection spectral characteristics, including polarization, of rock surface in 2π space by measuring and calculating the e and p values in several key directions.

Key words: model, reflection spectrum, rock, 2π space

1 Introduction

When using remote sensing data of multiple bands, multiple times and high spectra to enhance the discernibility for ground objects, scientists have noticed the influence and contribution of angle information to image recognition and classification. In fact, the angle information of objects is their three-dimensional spectral characteristics in 2π space. Researchers have put forward two methods to study angle spectral characteristics. The first one emphasizes application of the method, but ignores angle difference, assuming the object is a Lambert object. The other method emphasizes reality and differentiation of angle information and creates the bidirectional reflection distributing function (BRDF), which is defined as

$$\mathrm{BRDF}(i,r,\lambda)=\frac{\mathrm{d}I_r(\Omega_i,\Omega_r,\lambda)}{I_i(\Omega_i,\lambda)\cos\theta_i\mathrm{d}\Omega_i} \quad (1)$$

where I denotes radiance, subscripts *i and r* denote light of incidence and reflection respectively, λ is wavelength, Ω is the position angle, dependent on vertex angle (φ) and azimuth (θ). Formula 1 shows that the BRDF is a complex function that includes five variables (θ_i, φ_i, θ_r, φ_r and λ). This function clearly shows that reflective distribution is controlled by directions of both incidence and reflection, and that the objects have dissimilarities of three-dimensional spectra in 2π space. The formula, however, does not pay much attention to the spectral relationship of two neighboring points in three-dimensional space, so the method cannot express and illustrate the difference of the BRDF and the affiliation of two closing points when they have the same condition but a small differentiation of $\mathrm{d}\Omega$. Using the conception of the BRDF, we can do only point-by-point measurement of the BRDF in 2π space and thus this function has found only very poor application. At present, the ground object is still assumed to be a Lambert object in remote-sensing analysis.

This paper chooses the most common and important object on earth's surface—rock as a study sample. We measured and analyzed three-dimensional spectral characteristics of 20 sorts of rock in 2π space to find out the rule of the BRDF. The question is what characteristics the BRDF of rock has when a light beam irradiates the surface of the rock. As for this question, researchers have different viewpoints. Tong (1990) and others think that the reflection of surface rock is composed of mirror reflection and Lambert reflection, and usually one of them is dominant at a certain condition. However, an American scholar argues that "Deserving attention, in these curves, including any data curve of dry sand and soil, the reflectivity of mirror direction did not increase at all. In this way, it is unbelievable to describe these surface to suppose the total reflectivity was composed by mirror reflection and Lambert reflection" (Zhang, 2001). Obviously, different scholars have no congruous

viewpoint for this question.

2 Analysis of Reflection Spectra of Rock Surface in 2π Space

2.1 Influence of incidence angle on reflection spectra

Figures 1 and 2 are reflection spectra of basalt in 2π space at 760–1100 nm bands and the incidence angles are 20° and 60° respectively. In the figure, the abscissa denotes the azimuth (θ), from 0°–360° and different colors denote different vertex angles (φ), from 0–60°. In this way, all the data cover the 2π space of basalt's surface. The Y-coordinate denotes the light intensity of position angle.

As the American scholar points out, "According to the incidence angle's difference, the reflectivity varies correspondingly. But the attention which people paid to this question is less than the attention to reflection in 2π space" (Zhang, 2001). In fact, from Figs. 1 and 2 we can easily see that the spectral change of objects in 2π space is much obvious when the incidence angle is changing.

In Fig. 1, the curve of 20° (vertex angle) has no obvious wave crest in the mirror direction, but in Fig. 2 we found that curves with vertex angles of 30°, 40°, 50° and 60° have obvious wave crests in the mirror direction. Because of limited length of this paper, we cannot display the figures for incidence angles 10°, 30°, 40° and 50°. In fact, with the increase of incidence angle from 20° to 60°, the spectral curves of basalt in 2π space is changing gradually from Fig. 1 to Fig. 2.

From the above one can see that when the incidence angle is small (θ<20°) the reflection spectra of the rock surface are characterized by diffuse reflection and ther is almost no composite of mirror and diffuse reflections. This conclusion is consistent with the American scholar's. But when the incidence angle is big (θ >30°), the reflection spectra show a mirror reflection feature. In this case, it is reasonable to think that there is a composite of mirror and diffuse reflections. This conclusion is consistent with Tong and Tian's opinion (Tong et al., 1990). Thus, whether there is a composite of mirror reflection and diffuse reflection depends on the incidence angle.

2.2 Reflection spectral characteristics of rock surface in 2π space

Figure 1 shows that, when the incidence angle is small, the reflection spectra of rock in 2π space have no obvious difference, and thus the rock can be thought as a Lambert object. When the incidence angle is big, however, the reflection spectra of rock have strong characteristics of a non-Lambert object and the characteristics are closely related to the vertex angle. When the vertex angle is 0°, 10° or 20°, the reflection spectra have no change as the azimuth is changed. The rock keeps the Lambert characteristics and shows a nearly a straight line (theoretically, the curve corresponding to 0° is a utterly unbent line). We use the reflection spectral curve of vertex angle 10° in Fig. 2 to compile Fig. 3, which shows the relation between the intensity of reflection and the azimuths. The dots in the figure denote the observation values and the red line is the fitting circle with a radius of 0.804. The fitting is good enough.

When the vertex angle is 30°–60°, the spectral curves have no more Lambert characteristics. Because of the mirror effect, there appears a wave crest in the region of 160°–200°. The height of he wave crest changes according to the vertex angle. The curve for 30° has a relatively low crest, while those for 40°, 50° and 60° are fairly high. In the same way, we use the reflection spectral curve of vertex angle 60° from Fig. 2 to make Fig. 4, which shows the relation between the light intensity of reflection and the azimuth. In this case, the figure is more like an ellipse. Actually, the azimuth of 180° is the mirror direction. The phenomena indicates that the mirror effect of earth's surface is intensified when the vertex angle increases, thus destroying the ordinary Lambert characteristics.

Spectral analysis shows that the light intensities for vertex angles 0°, 10° and 20° have no obvious difference. The light intensity for 20° is the largest one, averaging 0.921 and that for 0° is the second largest one, whose average is 0.885. 0.804 is for 10° and those for 50° and 60° are rather small, whose gained energy is only half the case when the vertex angle is 20°.

The spectral curves for the other 19 sorts of rock exhibit the same characteristics as below. When the vertex angle is 0°, 10° or 20°, the reflection spectra have no change as the azimuth is changed. These curves have no undulation and are basically straight lines. When the vertex angle becomes larger, for example from 30° to 60°, the spectral curves have wave crests in the region of 160°–200°. The crest is changed with the vertex angle. And the line fitting the observed values (dots in the figure) is more like an ellipse.

From the above discussion we have reached the following conclusion. When the vertex angle is small, the reflection spectra still have the Lambert characteristics, whereas when the vertex angle is large the reflection spectra have no Lambert characteristics, representing a figure like an ellipse in this case.

We know the function $y=eP/(1+e\cos\theta)$ is an ellipse curve. In Fig. 5, we give six standard ellipse curves (P=8 and e=0.2, 0.4, 0.6, 0.7, 0.8 and 0.9 respectively). It can be seen by comparing Fig. 5 with Fig. 2 that these curves are very similar to each other. With the increase of

eccentricity, the wave crest rises quickly. The curves have slight undulation when $e<0.4$, but have obvious undulation when $e>0.6$.

As observing Fig. 2 and Fig. 5 carefully, one will find an obvious difference. In Fig. 5 the whole curves of small eccentricity are under those corresponding to large centricities, while in Fig. 2 some parts of the curves of small eccentricity are above the curves of large eccentricity. Then we drew curves of another standard ellipse with the product of e and p being a constant 1 (Fig. 6). At this time, the curves corresponding to small eccentricities are above those of large eccentricity.

2.3 Physical mechanism for the ellipse distribution of spectra of rock surfaces at the same vertex angle

What is the reason why the spectra of rock surfaces show ellipse distribution at the same vertex angle? In the case of composition by simply mirror reflection and diffuse reflection, there must exist jump discontinuities. In fact, the corresponding curve is increasing smoothly. What is the physical mechanism? We consider that usually the curve is a circle when the surface is a standard Lambert surface, but the mirror reflection elongates the circle at the mirror direction when the vertex angle becomes large.

We know that Maxwell's electromagnetic theory can deduce the Fresnel formula. But before the creation of Maxwell's electromagnetic theory (in 1823), A. J. Fresnel found the Fresnel formula by using the elastic wave theory. This inspires us to think that it reasonable to consider light as a sort of elastic matter, so the above question is similar to the case when a pair of force acts on an elastic circle with AB as the vertical diameter (radius is a). This is analogous to the case when mirror reflection is added to diffuse reflection. It can be proved that the circle will be distorted into an ellipse at this time. We cut the circle along AB, the shear forces of sections C and D are zeros (CD is perpendicular to AB) because of symmetrical load. There are only an axial force F_{N0} and a bending moment M_0. According to the balance condition, we can easily know that $F_{N0}=F/2$ and M_0 is the superfluous restraining force. Because the circle is balance for diameters AB and CD, so we can focus on a quarter of the circle (the first quadrant, arc DA). Because the rotation angles of sections A and D are zero, section A can be regarded as the fixed end while section D as the concordant condition of distortion. We, therefore, have

$$\delta_{11}M_0+\Delta_{1F}=0 \qquad (2)$$

In formula (2), Δ_{1F} is the rotation angle of section D in the basic static system when $F_{N0}=F/2$. δ_{11} is the rotation angle of section D when $M_0=1$ and the δ_{11} acts independently. Now we can calculate Δ_{1F} and δ_{11}. Defining the angle with the jumping-off line of OD to be f, we have

$$M=\frac{Fa}{2}(1-\cos\phi),\ M_1=-1,$$

$$\text{so } \Delta_{1F}=\int_0^{\frac{\pi}{2}}\frac{MM_1}{EI}a\mathrm{d}\phi=\frac{Fa^2}{2EI}\int_0^{\frac{\pi}{2}}(1-\cos\phi)(-1)\mathrm{d}\phi$$

$$=-\frac{Fa^2}{2EI}(\frac{\pi}{2}-1),$$

$$\text{and } \delta_{11}=\int_0^{\frac{\pi}{2}}\frac{M_1M_1}{EI}a\mathrm{d}\phi=\frac{a}{EI}\int_0^{\frac{\pi}{2}}(-1)^2\mathrm{d}\phi=\frac{\pi a}{2EI}$$

Substituting Δ_{1F} and δ_{11} in formula (2), we have $M_0=Fa(1/2-1/\pi)$.

After obtaining M_0, we can calculate the bending moment when $F/2$ and M_0 act together:

$$M(\phi)=\frac{Fa}{2}(1-\cos\phi)-Fa(\frac{1}{2}-\frac{1}{\pi})=Fa(\frac{1}{\pi}-\frac{\cos\phi}{2})$$

This bending moment is 1/4 of a circle. Under the bending moment, the circle is distorted to become an ellipse as the force is balance. We can measure the length change of AB at the force of F. The length change of AB is denoted with D_{AB}. Assuming $F=1$, we can obtain the bending moment $M_0(f)$ in this condition:

$$M_0(\phi)=a(\frac{1}{\pi}-\frac{\cos\phi}{2}) \qquad (0\le\phi\le\frac{\pi}{2})$$

By using the Moore integral, D_{AB}, the comparative displacement of A and B, is

$$\Delta_{AB}=4\int_0^{\frac{\pi}{2}}\frac{M(\phi)M_0(\phi)}{EI}a\mathrm{d}\phi$$

$$=\frac{4Fa^3}{EI}\int_0^{\frac{\pi}{2}}(\frac{1}{\pi}-\frac{\cos\phi}{2})^2\mathrm{d}\phi \qquad (3)$$

$$=\frac{Fa^3}{EI}(\frac{\pi}{4}-\frac{2}{\pi})$$

In formula (2), EI is the material's intension of resisting bend. The reason that the spectra of rocks have many different eccentricities of ellipses is that the incidence angles, vertex angle and the quality of rocks are all variable.

3 Influence of Rock Types on Rock Spectra

In Fig. 7 illustrates the spectrum of peridotite at the incidence angle of 50° in 2π space and Fig. 8 shows spectra of other materials than rocks (standard material; the main component is MgO) in the same condition. Comparing Fig. 2 and Fig. 5 with Fig. 8, we can se Fig. 2 and Fig. 5 have more similarities, although they represent

different rocks. There are wave crests in the region of 160° –200°. But in Fig. 8, the wave crest changes gently. The similarity shows that basalt and peridotite are both rocks, so their spectral curves are similar in 2π space. But their differences show that they are different rocks after all and have distinct components and material structures, so their spectral curves in 2π space have certain differences. These similarities and differences are very important and useful to prospecting of rock mineral resources and classification of rocks.

4 Conclusions

From the above discussion, it can be easily seen that the reflection spectra of rock surfaces are variable significantly with incidence angle, vertex angle, wave length and lithology. However, their reflection spectra still have some common rules.

(1) When the incidence angle is small, the reflection spectrum of rock surface in 2π space still has the Lambert characteristics. So as measure light intensities of only several different vertex angles, we can get the whole spectral characteristics of rock surface in 2π space.

(2) When the incidence angle is big, the reflection spectrum is a synthesis of mirror reflection and diffuse reflection. When the vertex angle is 0°, 10° and 20°, the spectral curves have no undulation, and are nearly straight lines. When the vertex angle becomes larger from 30° to 60°, the spectral curves have wave crests in the region of 160°–200°, and the shape of the curves is much like an ellipse. So we can measure and calculate the e and p values to describe the whole spectral characteristics of rock surface in 2π space.

(3) Different rocks have different e and p values, which can be used to identify the type of rocks. This thus provides a new approach to exploration of rock mineral resources and rock classification.

Manuscript received Nov. 7, 2003
accepted Nov. 20, 2003
edited by Liu Xinzhu

References

Bicheron, P., Leroy, M., and Hautecoeur, O., 1997. Enhanced discrimination of Boreal forest covers using directional signatures measured by the airborne POLDER instrument. *J. Remote Sensing*, 4(1): 106–110.

Fornaro, G., Serafino, F., and Soldovieri, F., 2003. Three-dimensional focusing with multipass SAR data. *IEEE Trans. on Geosci. Remote Sensing*. 41(3): 507–517.

Jin Xifeng, Qiao Delin and Zhou Dexiang (patentees), 1998. Patent No. 96239489.0. Changchun Institute of Fine Mechanics and Optics, Chinese Academy of Sciences.

Li Xiaowen and Strahler, A.H., 1985. Geometric optical modeling of a coniferous forest canopy. *IEEE Trans. Geosci. Remote Sensing*. 23: 207–221.

Slater, P.N., 1980. *Remote sensing optics and optical systems*. Boston: Addison-Wesley Published Company, 25–26.

Song Chunqing and Zhang Zhenchun, 1978. *Geology*. Beijing. People's Education Publishing House, 565 (in Chinese).

Tong Qingxi (editor in chief), 1990. *Spectra and Analysis of Typical Ground Objects in China*. Beijing: Science Press, 45–50 (in Chinese).

Yan Lei and Zhao Hu, 2000. Structure Control for the Huge System on Resources, Environment and Ecology. *Advances in Systems Science and Applications*, 2: 145–148.

Zhang Jingbo (ed.), 2001. *Method of Emendation for Remote Sensing Data*. Beijing: Aviation Industry Publishing House, 88–98 (in Chinese).

Zhang Zhixiang, 1985. *The Polarization of Light*. Beijing: Higher Education Publishing House, 1–5 (in Chinese).

Zhao Yunsheng, Huang Fang, Jin Lun, Jin Xifeng and Zhou Shuxiang, 2000. Study on polarizing reflectance characteristic of plant simple leaf. *J. Remote Sensing*, 4(2): 131–135 (in Chinese).

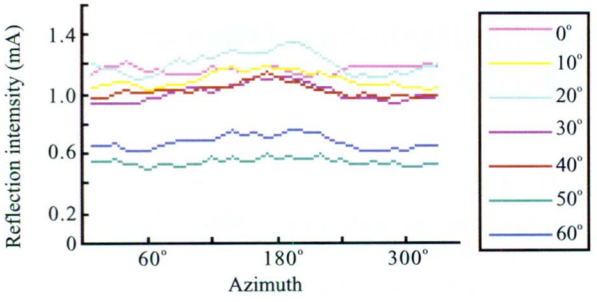

Fig.1. Spectrum curve of basalt.
Incidence angle=20°.

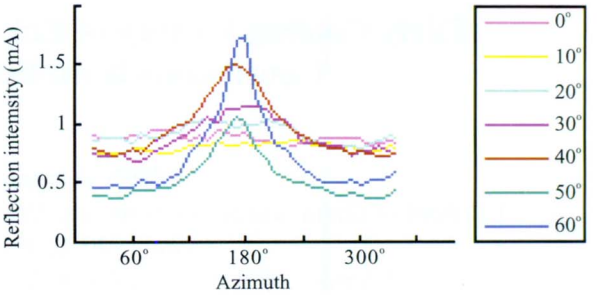

Fig.2. Spectrum curve of basalt.
Incidence angle=60°.

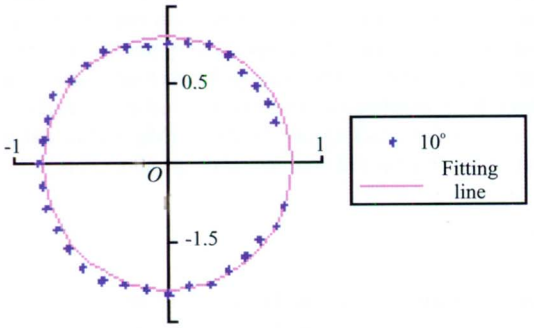

Fig.3. Reflection spectrum curve of vertex angle 10°.

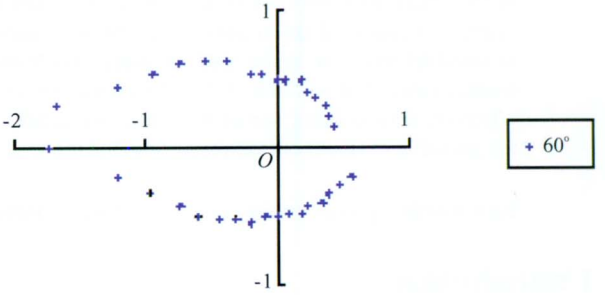

Fig.4. Reflection spectrum curve of vertex angle 60°.
Incidence angle=60°,760-1100 nm.

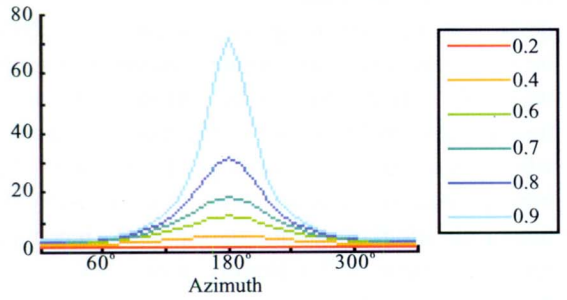

Fig.5. Standard ellipse curves, *P* unchanged.

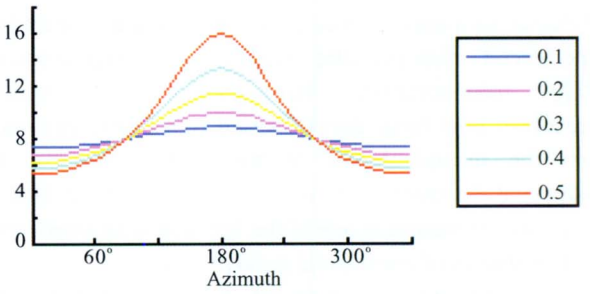

Fig.6. Standard ellipse curves, *eP* unchanged.

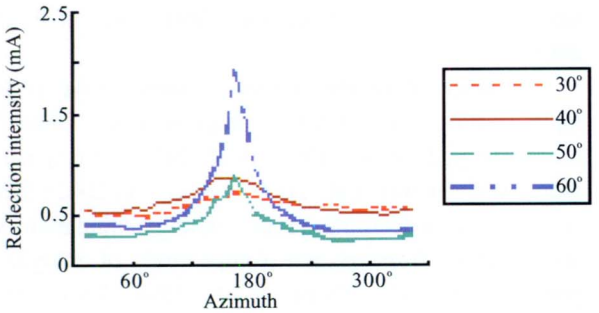

Fig.7. Spectral curves of peridotite in 2π space.

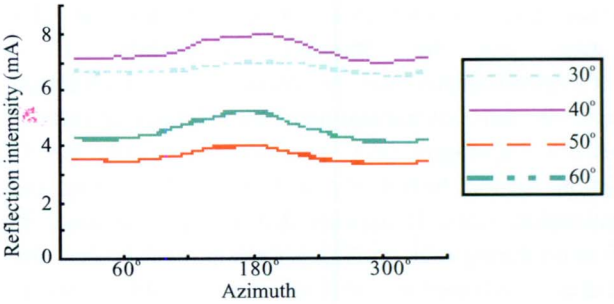

Fig.8. Spectral curves of MgO in 2π space.
Incidence angle=50°,760-1100 nm.